Letter

New solutions to the complex Ginzburg-Landau equations

Robert Conte [*]
Université Paris-Saclay, ENS Paris-Saclay, CNRS, Centre Borelli, F-91190 Gif-sur-Yvette, France and Department of Mathematics, The University of Hong Kong, Pokfulam, Hong Kong

Micheline Musette [†]
Dienst Theoretische Natuurkunde, Vrije Universiteit Brussel, Pleinlaan 2, B-1050 Brussels, Belgium

Tuen Wai Ng [‡]
Department of Mathematics, The University of Hong Kong, Pokfulam, Hong Kong

Chengfa Wu [§]
Institute for Advanced Study, Shenzhen University, Shenzhen, People's Republic of China

(Received 8 June 2022; accepted 31 August 2022; published 7 October 2022)

The various regimes observed in the one-dimensional complex Ginzburg-Landau equation result from the interaction of a very small number of elementary patterns such as pulses, fronts, shocks, holes, and sinks. Here we provide three exact such patterns observed in numerical calculations but never found analytically. One is a quintic case localized homoclinic defect, observed by Popp *et al.* [S. Popp *et al.*, Phys. Rev. Lett. **70**, 3880 (1993)], and the two others are bound states of two quintic dark solitons, observed by Afanasyev *et al.* [V. V. Afanasyev *et al.*, Phys. Rev. E **57**, 1088 (1998)].

DOI: 10.1103/PhysRevE.106.L042201

I. INTRODUCTION

Slowly varying amplitudes of numerous physical phenomena evolve in time according to the ubiquitous one-dimensional complex Ginzburg-Landau (CGL) equation,

$$iA_t + pA_{xx} + q|A|^2A + r|A|^4A - i\gamma A = 0, \tag{1}$$

in which the constants p, q, r are complex and γ is real. These phenomena include pattern formation, spatiotemporal intermittency, superconductivity, nonlinear optics, Bose-Einstein condensation, etc.; see the reviews [1,2].

In the cubic case ($r = 0$), it describes, for instance, the formation of patterns near a Hopf bifurcation (γ being the distance from criticality) to an oscillatory state. The regimes are extremely rich and, depending on the parameters, range from chaotic (turbulent) to regular (laminar); see the phase diagrams in the plane $[\mathrm{Re}(p)/\mathrm{Im}(p), \mathrm{Re}(q)/\mathrm{Im}(q)]$ [3, Fig. 1] [4, Fig. 1(a)]. The observed patterns have been classified [5, Fig. 1] according to both their homoclinic (equal values of $\lim_{x\to-\infty}|A|$ and $\lim_{x\to+\infty}|A|$) or heteroclinic (unequal values) nature, and their topology: pulses, fronts, shocks, holes, and sinks. For instance, the holes (characterized by the existence of a minimum of $|A|$) can be either heteroclinic (such as the analytic solution of Bekki and Nozaki [6]) or homoclinic (as displayed by numerical simulations of van Hecke [4]). Of particular interest is the case when $|A|$ can vanish; since the phase $\arg A$ is then undefined, it can undergo discontinuities, a feature which creates topological defects. This "defect-mediated turbulence" [7] [8] is a major mechanism [9] of transition to a turbulent state, in addition to the mechanism of phase turbulence.

The situation is similar in the complex quintic case (CGL5, r/p not real) [5], and the importance of these coherent structures is their role of separators between different regimes; cf. [5, Figs. 5,6]. All these coherent structures are indeed observed both in physical phenomena and in numerical simulations [3,4].

In Taylor-Couette flows between rotating or counter-rotating cylinders [10], when a parameter varies, one first observes the expected Benjamin-Feir instability, followed by the occurrence of spatiotemporal defects (i.e., a vanishing of $|A|$, which allows a discontinuity in the phase of A) and a large variation of the amplitude. A similar behavior is also observed in Rayleigh-Bénard convection (a fluid between two conducting plates, heated from below) [11].

In nonlinear optics where t is a coordinate along the fiber and x a transverse coordinate, the goal is to carefully select the initial signal (for instance, one of the coherent structures) and to tune the parameters of the CGL equation in order to minimize the attenuation during the propagation of this signal. Various kinds of bright or dark solitons, or more general "dissipative" solitons, can be used for this purpose [12–14].

*Robert.Conte@cea.fr
†Micheline.Musette@gmail.com
‡NTW@maths.hku.hk
§CFWu@szu.edu.cn

There also exist other optical devices described by a system [15, Eqs. (1)–(3)] involving a CGL-like equation for the electric field. In these broad area, vertical cavity surface-emitting lasers (VCSELs) with a single longitudinal mode, two transverse coordinates (among them our x) are necessary to describe the broad area and one observes, for instance, various patterns similar to those in spatiotemporal intermittency [16,17].

From a more general point of view, there is a strong evidence [18] that coherent structures govern the transition between different scenarios of chaos.

Of special interest to our purpose is the fact that some of the observed patterns have been represented by exact, closed form, analytic expressions, such as the CGL5 heteroclinic hole [6], a traveling wave with arbitrary velocity. Conversely, it is reasonable to believe that every elementary observed pattern could be associated to some analytic solution, to be found; this is the motivation of the present work.

In this Letter, we consider the most challenging situation, i.e., the so-called complex cases in which r/p is not real and, if r vanishes, q/p is not real, respectively denoted CGL5 and CGL3. This excludes the nonlinear Schrödinger (NLS) limit (p, q real, γ zero), which does not display any chaotic regime. Our interest is to look for exact traveling wave solutions (c and ω real),

$$A = \sqrt{M(\xi)}e^{i[-\omega t + \varphi(\xi)]},\ \xi = x - ct. \tag{2}$$

Such traveling waves are characterized by a third-order nonlinear ordinary differential equation (ODE); see (3) hereafter.

The current list of exact traveling waves is very short and comprises only six solutions [19]: for CGL3, a homoclinic pulse [20], a heteroclinic front [21], a heteroclinic source or hole [6] [22, Fig. 5]; for CGL5, a homoclinic pulse [5], a heteroclinic front [5], a homoclinic. source or sink [23,24]. Other elementary patterns exist, but they have only been observed experimentally, an important one being a CGL3 homoclinic hole [4] [25, Fig. 1(b)].

A lot of effort has been devoted to the search for exact solutions of CGL3/5, by essentially three methods, which we now outline. A slight modification of the method of Hirota allowed Bekki and Nozaki [6,21] to uncover two of the three above-mentioned traveling waves of CGL3. By making heuristic assumptions among the components of a three-dimensional dynamical system equivalent to (3), van Saarloos and Hohenberg [5, Sec. 3.3] succeeded in obtaining two remarkable solutions of CGL5: the pulse and the front solutions. In the third method, building on previous work [26], Marcq *et al.* [24] made an assumption for the complex amplitude A matching the structure of singularities [27] and thus found the full CGL5 source or sink.

In the present work, by combining two mathematical methods, we present new traveling waves, outlined in [27], and moreover we prove that these are the only ones whose square modulus $M(\xi)$ admits only poles as singularities in the complex plane of ξ (in short, is *meromorphic* on $\mathbb{C}$). Each such meromorphic solution is characterized by a first-order nonlinear ODE for $M(\xi)$.

Only three of these new solutions are bounded; they are all homoclinic, decrease exponentially fast to a constant value at infinity, and only exist for CGL5. One represents a topological defect, previously observed experimentally [28, Fig. 3(b)] [29, Fig. 4] for a set of parameters compatible with ours. The two other traveling waves are bound states made of two CGL5 dark solitons; while in CGL3 the presence of sources inhibits the formation of bound states of dark solitons [30], such bound states have been numerically observed in CGL5 by Afanasjev *et al.* [30, Fig. 4] and, more recently, in [31, Fig. 3(d)].

The three other solutions, outlined in [27] (one doubly periodic for CGL3, one doubly periodic and one rational for CGL5), are unbounded, but, under a small perturbation which moves the poles outside the real axis $x - ct$, their analytic expression becomes bounded and the corresponding periodic patterns could be good approximations of a variety of periodic patterns observed experimentally; this is currently under investigation.

In the next section, we simply outline the mathematics involved. Then, for each bounded solution, the amplitude A is presented as a product of complex powers of entire functions.

II. THE METHOD

The method arises from a simple remark: in all presently known exact traveling waves (six, recalled above), the only singularities of the square modulus $|A|^2 = M$ in the complex plane of ξ are poles. Conversely, let us make the *only* assumption that $M(\xi)$ is meromorphic on $\mathbb{C}$.

First, using Nevalinna theory [32], it has been proven [33] that for all values of the CGL parameters p, q, r (complex), γ (real) and of the traveling waves' parameters c, ω (real), for both CGL3 and CGL5, all solutions $M(\xi)$ meromorphic on $\mathbb{C}$ are elliptic or degenerate elliptic and therefore obey a nonlinear ODE of first order.

As a consequence, in order to find all meromorphic solutions of both CGL3 and CGL5, only a finite number of possibilities need to be examined. This is done by two methods. The first method (Hermite decomposition [34]) represents M as a finite sum of derivatives of "simple elements" admitting only one pole of residue unity [Weierstrass' $\zeta(\xi)$ [35] or its degeneracies $k\coth(k\xi)$ and $1/\xi$], while the second one (subequation method [36,37]) builds the first-order ODE obeyed by $M(\xi)$ and then integrates it. Full details can be found in [27].

The modulus $M(\xi)$ obeys a third-order ODE [36],

$$\begin{aligned}
&(G' - 2\kappa_i G)^2 - 4GM^2(e_iM^2 + d_iM - g_r)^2 = 0,\\
&G = \frac{MM''}{2} - \frac{M'^2}{4} - \frac{\kappa_i}{2}MM' + g_iM^2 + d_rM^3 + e_rM^4,\\
&\varphi' = \frac{\kappa_r}{2} + \frac{G' - 2\kappa_i G}{2M^2(g_r - d_iM - e_iM^2)},
\end{aligned} \tag{3}$$

in which the real parameters $d_r, d_i, e_r, e_i, \kappa_r, \kappa_i, g_r, g_i$ are

$$\begin{aligned}
&\frac{q}{p} = d_r + id_i,\ \frac{r}{p} = e_r + ie_i,\ \frac{c}{p} = \kappa_r - i\kappa_i,\\
&\frac{\gamma + i\omega}{p} = g_r + ig_i - \frac{1}{2}\kappa_r\kappa_i - \tfrac{i}{4}\kappa_r^2.
\end{aligned} \tag{4}$$

This ODE is the key to obtain all meromorphic solutions $M(\xi)$ and, by the quadrature $(3)_3$, the complex amplitude A. These solutions occur for specific values of d_r/d_i (CGL3) and

e_r/e_i (CGL5), which characterize the local behavior of $Ae^{i\omega t}$ near a movable singularity ξ_0 (i.e., whose location depends on the initial conditions) [24,38],

$$Ae^{i\omega t} \sim \begin{cases}(\text{CGL3})\ A_0(\xi-\xi_0)^{-1+i\alpha},\\ (\text{CGL5})\ A_0(\xi-\xi_0)^{-1/2+i\alpha},\end{cases} \quad \alpha \text{ real.} \tag{5}$$

III. THE NEW ANALYTIC PATTERNS

A. CGL5, localized homoclinic defect

For the parameters

$$\kappa_{\rm i}=0,\ \frac{e_r}{e_i}=\frac{3}{2},\ \frac{d_r}{d_i}=\frac{29}{15},\ \frac{g_r}{g_i}=-\frac{12}{35},\ g_i=\frac{7d_i^2}{12e_i}, \tag{6}$$

there exists a first-order subequation,

$$\left[M'^2+e_iM\left(M+\frac{2d_i}{3e_i}\right)P_2\right]^2-\frac{4}{3}e_i^2M^2P_2^3=0,$$
$$P_2=M^2+\frac{6d_i}{5e_i}M+\frac{d_i^2}{3e_i^2}, \tag{7}$$

in which a rescaling of M and ξ leaves no arbitrariness. If p is not real, as usually assumed so as to be far away from the integrable nonlinear Schrödinger situation, this pattern is stationary ($c=0$); otherwise it is moving with an arbitrary velocity c.

In the original notation (p,q,r,γ,c,ω), the parameters obey the constraints

$$cp_i=0,\ \frac{p_rr_r+p_ir_i}{p_rr_i-p_ir_r}=\frac{3}{2},\frac{p_rq_r+p_iq_i}{p_rq_i-p_iq_r}=\frac{29}{15},$$
$$\gamma=\frac{(p_rq_i-p_iq_r)^2}{|p|^2(p_rr_i-p_ir_r)}\left(-\frac{7}{12}p_i-\frac{1}{5}p_r\right),$$
$$\omega=\frac{(p_rq_i-p_iq_r)^2}{|p|^2(p_rr_i-p_ir_r)}\left(\frac{7}{12}p_r-\frac{1}{5}p_i\right)-\frac{p_r^3}{4|p|^4}c^2. \tag{8}$$

The solution of this subequation [the invariance of (3) by translation allows us to set $\xi_0=0$],

$$M=-20\frac{d_i}{e_i}\frac{\coth^2\frac{k\xi}{2}\left(\coth^2\frac{k\xi}{2}-1\right)}{\left(5\coth^2\frac{k\xi}{2}-3\right)^2-12},$$
$$k^2=\frac{d_i^2}{15e_i}=\frac{(p_rq_i-p_iq_r)^2}{15(p_rr_i-p_ir_r)|p|^2}, \tag{9}$$

displays four simple poles $\pm\xi_A,\pm\xi_B$,

$$\coth\frac{k\xi_A}{2}=\frac{\sqrt{10\sqrt{3}+15}}{5},\quad \coth\frac{k\xi_B}{2}=\frac{\sqrt{10\sqrt{3}-15}}{5}i, \tag{10}$$

and a shift of $k\xi/2$ by one half-period $i\pi/2$ (equivalent to permuting cosh and sinh) makes M bounded for $e_i=\text{Im}(r/p)>0$. In order to deduce the complex amplitude, one computes the logarithmic derivative $d\log(Ae^{i\omega t})/d\xi$ with A defined by (2). By virtue of $(3)_3$, this is a rational function of $\coth(k\xi/2)$, whose Hermite decomposition [34] is a finite sum of shifted coth. Then its logarithmic primitive yields the complex amplitude A as the product of powers of five sinh functions,

$$\frac{A}{A_0}=e^{-i\omega t+i\frac{\kappa_{\rm r}}{2}\xi}\sinh\frac{k\xi}{2}$$
$$\times\left(\sinh\frac{k(\xi-\xi_A)}{2}\sinh\frac{k(\xi+\xi_A)}{2}\right)^{\frac{-1+(3+2\sqrt{3})i}{2}}$$
$$\times\left(\sinh\frac{k(\xi-\xi_B)}{2}\sinh\frac{k(\xi+\xi_B)}{2}\right)^{\frac{-1+(3-2\sqrt{3})i}{2}}. \tag{11}$$

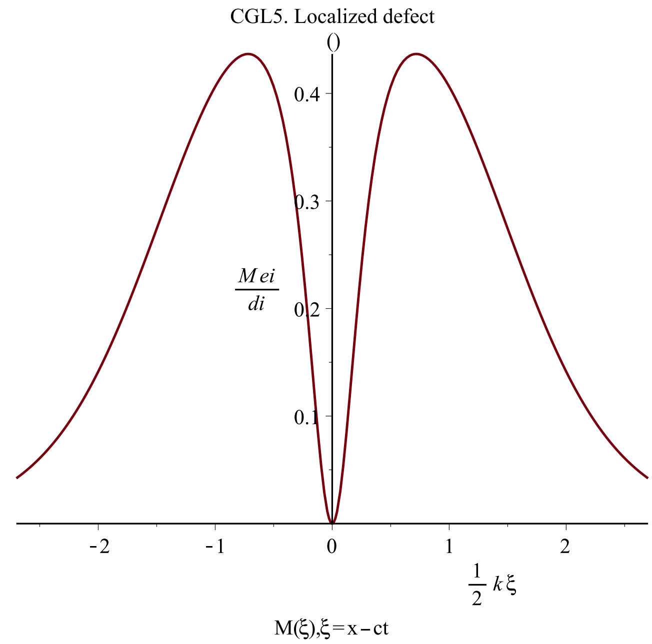

FIG. 1. CGL5. Homoclinic defect in dimensionless units $M/(d_i/e_i)$ vs $k\xi/2$.

The modulus M displays a unique minimum $M=0$. This new analytic pattern decreases exponentially fast at infinity, has the topology of a double pulse (Fig. 1), and is an exact representation of a defect in CGL. The study of its stability under small perturbations has not been performed in this Letter; this will be investigated later.

Although defect-mediated turbulence is mainly observed in two-dimensional CGL3 where this is a major mechanism of turbulence [39] [22], it has also been reported in CGL5 [28, Fig. 3b] [29, Fig. 4] [22, p 278], where, for a destabilizing CGL5 term (negative δ in the notation of Ref. [28]) compatible with the present numerical values (6), one observes a succession of phase slips (every time M vanishes), which create hole-shock collisions, ending in a process of as many annihilations as creations. Such a process is known as "hole-mediated turbulence." We must also mention that a pattern topologically identical to the present defect has been numerically observed in a system of two amplitude equations coupled quadratically [40, Fig. 2].

This exact pattern should be quite useful for determining the range of parameters for which topologically similar patterns are stable or metastable. Indeed, choosing as the initial data an analytic expression similar to (11), appropriate sets of parameters of CGL5 should considerably shorten the duration of the transient regime and accordingly increase the convergence towards a topologically similar pattern.

B. CGL5, bound state of two dark solitons

When e_r/e_i is one of the four real roots of

$$1089 - 81\,327\lambda^2 + 323\,512\lambda^4 + 456\,976\lambda^6 = 0,$$
$$\lambda = \frac{e_r}{e_i},\ \lambda = \pm 0.1192,\ \lambda = \pm 0.4300, \tag{12}$$

there also exists a four-pole subequation (see Appendix for its coefficients) without any free parameter. To each of these four values of $\lambda = e_r/e_i$ correspond two values α_1, α_2 of the exponent α defined in (5), whose product is $\alpha_1\alpha_2 = -3/4$,

$$\lambda = \frac{e_r}{e_i} = \frac{\alpha}{2} - \frac{3}{8\alpha},$$
$$\lambda = \pm 0.1192,\ \alpha = (\mp 0.7550, \pm 0.9934),$$
$$\lambda = \pm 0.4300,\ \alpha = (\mp 0.5369, \pm 1.397). \tag{13}$$

The derivation of M, then A, follows exactly the same logic as for the defect solution. The complex amplitude A is the product of powers of six sinh functions,

$$\frac{A}{A_0} = e^{-i\omega t + i\frac{\kappa_r}{2}\xi} \times \sinh\frac{k(\xi-\xi_N)}{2}\sinh\frac{k(\xi+\xi_N)}{2}$$
$$\times\left(\sinh\frac{k(\xi-\xi_A)}{2}\sinh\frac{k(\xi+\xi_A)}{2}\right)^{-\frac{1}{2}+i\alpha_1}$$
$$\times\left(\sinh\frac{k(\xi-\xi_B)}{2}\sinh\frac{k(\xi+\xi_B)}{2}\right)^{-\frac{1}{2}+i\alpha_2}. \tag{14}$$

The zeros $(\pm\xi_A, \pm\xi_B)$ have their squares real and are the poles of M; the other zeros $(\pm\xi_N)$ and their complex conjugates $\pm\overline{\xi_N}$ are the four zeros of M,

$$M = M_0 + \frac{d_i}{e_i}\frac{\left(K_1\coth^2\frac{k\xi}{2} + K_2\right)\left(\coth^2\frac{k\xi}{2} - 1\right)}{\coth^4\frac{k\xi}{2} + D_1\coth^2\frac{k\xi}{2} + D_0}. \tag{15}$$

This defines two similar-looking (but different) homoclinic patterns in the shape of a double well, whose aspect ratios [min(M):$\lim_{\xi\to\pm\infty} M$:max(M)] are (1:7.46:11.5) (Fig. 2) and (1:1.09:1.23) (Fig. 3).

Like for the defect pattern, these two patterns are stationary if p is not real and they move with an arbitrary velocity if p is real. They compare, at least qualitatively, quite well with the bound state of two CGL5 dark solitons, as reported in [30, Fig. 4].

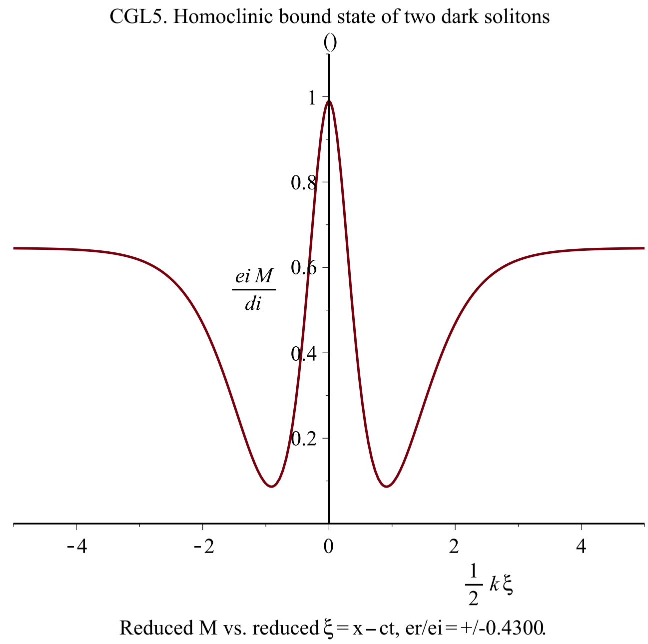

FIG. 2. CGL5. The homoclinic bound state in dimensionless units $M/(d_i/e_i)$ vs $k\xi/2$, for $\lambda = \pm 0.4300$, with aspect ratio (1:7.46:11.5).

IV. CONCLUSION

On the numerical side, these exact patterns can be used as building blocks to study the interaction of defects and dark

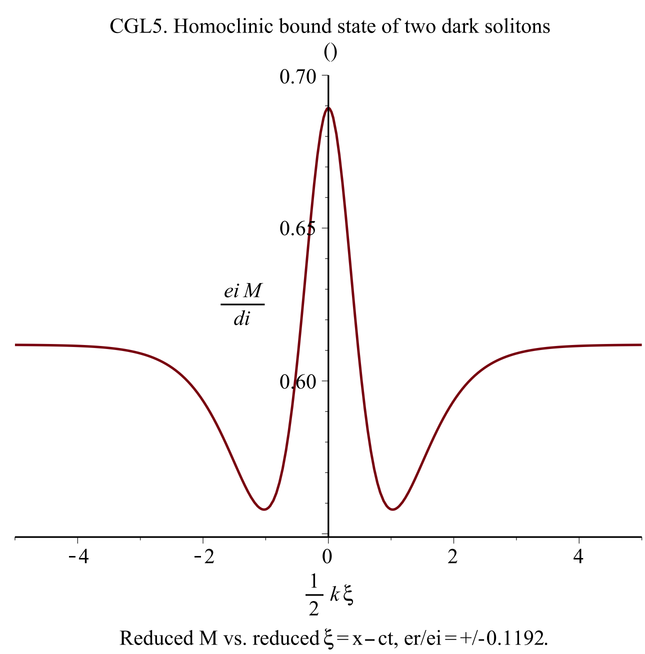

FIG. 3. CGL5. The homoclinic bound state in dimensionless units $M/(d_i/e_i)$ vs $k\xi/2$, for $\lambda = \pm 0.1192$, with aspect ratio (1:1.09:1.23).

solitons with various other patterns. On the analytic side, more exact traveling waves (with less constraints on $p, q, r, \gamma, c, \omega$) would necessarily be nonmeromorphic; this question will be addressed in future work.

ACKNOWLEDGMENTS

The authors warmly thank Joceline Lega for sharing her expertise. R.C. and M.M. thank CIRM, Marseille (Grant No. 2311) and IHES, Bures-sur-Yvette for their hospitality. T.W.N. was partially supported by the RGC Grant No. 17307420. C.W. was supported by the National Natural Science Foundation of China (Grant No. 11701382).

APPENDIX: DETAILS OF CGL5 TWO HOMOCLINIC BOUND STATES

The subequation has the structure

$$\begin{aligned}
&\left[M'^2 + c_6 P_{2a}(M) P_{2b}(M)\right]^2 - c_7 P_1(M)^2 P_{2a}(M)^3 = 0,\\
&\kappa_{\rm i} = 0,\ P_1(M) = M + c_1,\\
&P_{2a}(M) = M^2 + c_2 M + c_3,\ P_{2b}(M) = M^2 + c_4 M + c_5,
\end{aligned} \tag{A1}$$

with P_1, P_{2a}, P_{2b} polynomials and c_j constants.

Let us choose e_i and d_i as scaling parameters. The fixed parameters, as well as three movable constants, are polynomials of e_r/e_i (denoted λ),

$$\begin{aligned}
d_r &= d_i \lambda \frac{828\,038\,745\,921 + 7\,649\,070\,764\,998\lambda^2 + 9\,025\,535\,790\,856\lambda^4}{1\,386\,644\,084\,775},\\
g_r &= \frac{d_i^2}{e_i} \frac{-58\,513\,290\,148\,629\,717 + 1\,113\,015\,753\,503\,375\,224\lambda^2 + 1\,243\,896\,610\,551\,884\,848\lambda^4}{178\,728\,931\,719\,095\,040},\\
g_i &= \frac{d_i^2}{e_i}\lambda \frac{119\,473\,478\,956\,925\,997 - 1\,651\,180\,178\,874\,084\,664\lambda^2 - 1\,567\,990\,451\,264\,571\,568\lambda^4}{1\,608\,560\,385\,471\,855\,360},\\
k^2 &= \frac{d_i^2}{e_i}\lambda \frac{470\,354\,925\,826\,628\,997 + 16\,800\,138\,410\,952\,093\,392\lambda^4 + 15\,744\,055\,491\,100\,758\,536\lambda^2}{2\,010\,700\,481\,839\,819\,200},\\
M_0 &= \frac{d_i}{e_i} \frac{-344\,373\,082\,347 + 2\,958\,053\,216\,864\lambda^2 + 3\,382\,994\,698\,928\lambda^4}{493\,029\,007\,920},\\
&\frac{\coth_A}{\coth_B} + \frac{\coth_B}{\coth_A} = 2i\sqrt{3}\lambda \frac{16\,223\,643 - 41\,722\,436\lambda^2 - 37\,472\,032\lambda^4}{6\,800\,175},
\end{aligned} \tag{A2}$$

but $\coth_A = \coth(\xi_A/2)$, $\coth_B = \coth(\xi_B/2)$ and the four parameters K_1, K_2, D_0, D_1 of (15) are algebraic functions of λ. They are obtained by equating the rational function (15) and the Hermite decomposition (sum of four simple poles),

$$\begin{cases}
K_1 = -\dfrac{k e_i}{d_i}(a_2 \coth_A + b_2 \coth_B),\ b_2 = \dfrac{i\sqrt{3}}{e_i a_2},\\
K_2 = \dfrac{k e_i}{d_i}(a_2/\coth_A + b_2/\coth_B)(\coth_A \coth_B)^2,\\
D_0 = \coth_A^2 \coth_B^2,\\
D_1 = -(\coth_A^2 + \coth_B^2).
\end{cases} \tag{A3}$$

All numerical values characterizing the two bound state solutions are listed in Table I.

TABLE I. CGL5 $\kappa_{\rm i} = 0$. Numerical values of the two homoclinic bound states. e_i and d_i are arbitrary real (scaling).

Variable	1	2
$e_r/e_i = \lambda$	± 0.4300	± 0.1192
d_r/d_i	0.7910	0.08068
$g_r e_i/d_i^2$	1.062	-0.2375
$g_i e_i/d_i^2$	∓ 0.06400	± 0.007092
α_1	∓ 0.5369	∓ 0.7550
α_2	± 1.397	± 0.9934
$\coth(k\xi_A/2)$	-0.6093 i	-0.8861 i
$\coth(k\xi_B/2)$	1.259	1.401
$\coth(k\xi_N/2)$	0.7331	2.319
(continued)	-0.1430 i	$+2.098i$
$(a_2 e_i/d_i)k$	0.9531 i	-0.2499 i
$M_0 e_i/d_i$	0.6454	-0.6118
K_1	-2.517	0.6230
K_2	0.2024	-0.1193
D_1	-1.215	-1.178
D_0	-0.5889	-1.541

[1] I. S. Aranson and L. Kramer, The world of the complex Ginzburg-Landau equation, Rev. Mod. Phys. **74**, 99 (2002).

[2] W. van Saarloos, Front propagation into unstable states, Phys. Rep. **386**, 29 (2003).

[3] H. Chaté, Spatiotemporal intermittency regimes of the one-dimensional complex Ginzburg-Landau equation, Nonlinearity **7**, 185 (1994).

[4] M. van Hecke, Building Blocks of Spatiotemporal Intermittency, Phys. Rev. Lett. **80**, 1896 (1998).

[5] W. van Saarloos and P. C. Hohenberg, Fronts, pulses, sources and sinks in generalized complex Ginzburg-Landau equations, Physica D **56**, 303 (1992); Erratum **69**, 209 (1993).

[6] N. Bekki and K. Nozaki, Formations of spatial patterns and holes in the generalized Ginzburg-Landau equation, Phys. Lett. A **110**, 133 (1985).

[7] P. Coullet, L. Gil, and J. Lega, Defect-Mediated Turbulence, Phys. Rev. Lett. **62**, 1619 (1989).

[8] M. van Hecke and M. Howard, Ordered and Self-Disordered Dynamics of Holes and Defects in the One-Dimensional Complex Ginzburg-Landau Equation, Phys. Rev. Lett. **86**, 2018 (2001).

[9] B. I. Shraiman, A. Pumir, W. van Saarloos, P. C. Hohenberg, H. Chaté, and M. Holen, Spatiotemporal chaos in the one-dimensional complex Ginzburg-Landau equation, Physica D **57**, 241 (1992).

[10] N. Latrache, N. Abcha, O. Crumeyrolle, and I. Mutabazi, Defect-mediated turbulence in ribbons of viscoelastic Taylor-Couette flow, Phys. Rev. E **93**, 043126 (2016).

[11] P. Manneville, *Dissipative Structures and Weak Turbulence* (Academic Press, Boston, 1990); French adaptation: *Structures dissipatives, chaos et turbulence* (Aléa-Saclay, Gif-sur-Yvette, 1991).

[12] Y. S. Kivshar and G. P. Agrawal, *Optical Solitons: From Fibers to Photonic Crystals* (Academic, San Diego, 2003).

[13] J. V. Moloney and A. C. Newell, *Nonlinear Optics* (CRC, Boca Raton, FL, 2004).

[14] *Dissipative Solitons: From Optics to Biology and Medicine*, Lecture Notes in Physics, Vol. 751, edited by N. Akhmediev and A. Ankiewicz (Springer, NY, 2008).

[15] X. Hachair, F. Pedaci, E. Caboche, S. Barland, M. Giudici, J. R. Tredicce, F. Prati, G. Tissoni, R. Kheradmand, L. A. Lugiato, I. Protsenko and M. Brambilla, Cavity solitons in a driven VCSEL above threshold, IEEE J. Select. Topics Quantum Electron. **12**, 339 (2006).

[16] S. Coulibaly, M. G. Clerc, F. Selmi and S. Barbay, Extreme events following bifurcation to spatiotemporal chaos in a spatially extended microcavity laser, Phys. Rev. A **95**, 023816 (2017).

[17] C. Rimoldi, M. Eslami, F. Prati and G. Tissoni, Extreme events in a broad-area semiconductor laser with coherent injection, Phys. Rev. A **105**, 023525 (2022).

[18] L. Brusch, M. G. Zimmermann, M. van Hecke, M. Baer, and A. Torcini, Modulated Amplitude Waves and the Transition from Phase to Defect Chaos, Phys. Rev. Lett. **85**, 86 (2000).

[19] R. Conte and M. Musette, Solitary waves of nonlinear nonintegrable equations, *Dissipative Solitons*, edited by N. Akhmediev and A. Ankiewicz, Lect. Notes Phys. **661**, 373 (2005).

[20] L. M. Hocking and K. Stewartson, On the nonlinear response of a marginally unstable plane parallel flow to a two-dimensional disturbance, Proc. R. Soc. London A **326**, 289 (1972).

[21] K. Nozaki and N. Bekki, Exact solutions of the generalized Ginzburg-Landau equation, J. Phys. Soc. Jpn. **53**, 1581 (1984).

[22] J. Lega, Traveling hole solutions of the complex Ginzburg-Landau equation: A review, Physica D **152-153**, 269 (2001).

[23] J. D. Moores, On the Ginzburg-Landau laser mode-locking model with fifth-order saturable absorber term, Opt. Commun. **96**, 65 (1993).

[24] P. Marcq, H. Chaté and R. Conte, Exact solutions of the one-dimensional quintic complex Ginzburg-Landau equation, Physica D **73**, 305 (1994).

[25] Y. Uchiyama and H. Konno, Velocity fluctuation of hole in 1D defect turbulence, Proceedings of the ISCIE International Symposium on Stochastic Systems Theory and its Applications **2014**, 356 (2014).

[26] R. Conte and M. Musette, Linearity inside nonlinearity: Exact solutions to the complex Ginzburg-Landau equation, Physica D **69**, 1 (1993).

[27] R. Conte and M. Musette, *The Painlevé Handbook*, Mathematical Physics Studies (Springer Nature, Switzerland, 2020), pp. xxxi–389.

[28] S. Popp, O. Stiller, I. Aranson, A. Weber and L. Kramer, Localized Hole Solutions and Spatiotemporal Chaos in the 1D Complex Ginzburg-Landau Equation, Phys. Rev. Lett. **70**, 3880 (1993).

[29] S. Popp, O. Stiller, I. Aranson and L. Kramer, Hole solutions in the 1d complex Ginzburg-Landau equation, Physica D **84**, 398 (1995).

[30] V. V. Afanasjev, P. L. Chu and B. A. Malomed, Bound states of dark solitons in the quintic Ginzburg-Landau equation, Phys. Rev. E **57**, 1088 (1998).

[31] M. A. Viscarra and D. Urzagasti, Dark soliton solutions of the cubic-quintic complex Ginzburg-Landau equation with high-order terms and potential barriers in normal-dispersion fiber lasers, J. Nonlinear Optic. Phys. Mater. **31**, 2250003 (2022).

[32] I. Laine, *Nevanlinna Theory and Complex Differential Equations* (de Gruyter, Berlin, 1992).

[33] R. Conte and T. W. Ng, Meromorphic traveling wave solutions of the complex cubic-quintic Ginzburg-Landau equation, Acta Applic. Math. **122**, 153 (2012).

[34] C. Hermite, Remarques sur la décomposition en éléments simples des fonctions doublement périodiques, Annales de la faculté des sciences de Toulouse II, C1 (1888) *Oeuvres d'Hermite*, Vol. IV, pp. 262–273. http://www.numdam.org/item/AFST_1888_1_2__C1_0/.

[35] M. Abramowitz and I. Stegun, *Handbook of Mathematical Functions*, 10th ed. (Dover, New York, 1972).

[36] M. Musette and R. Conte, Analytic solitary waves of nonintegrable equations, Physica D **181**, 70 (2003).

[37] R. Conte and M. Musette, Elliptic general analytic solutions, Stud. Appl. Math. **123**, 63 (2009).

[38] F. Cariello and M. Tabor, Painlevé expansions for nonintegrable evolution equations, Physica D **39**, 77 (1989).

[39] J. Lega, Défauts topologiques associés à la brisure de l'invariance de translation dans le temps, Ph.D. thesis, Université de Nice, 1989.

[40] S. Darmanyan, L. Crasovan and F. Lederer, Double-hump solitary waves in quadratically nonlinear media without loss and gain, Phys. Rev. E **61**, 3267 (2000).